

## About the validity of complex mass scheme for the $\Delta$ resonance and higher energy region approaches

This content has been downloaded from IOPscience. Please scroll down to see the full text.

2015 J. Phys. G: Nucl. Part. Phys. 42 105104

(<http://iopscience.iop.org/0954-3899/42/10/105104>)

View [the table of contents for this issue](#), or go to the [journal homepage](#) for more

Download details:

IP Address: 163.10.1.243

This content was downloaded on 10/09/2015 at 14:06

Please note that [terms and conditions apply](#).

# About the validity of complex mass scheme for the $\Delta$ resonance and higher energy region approaches

C Barbero<sup>1,2</sup> and A Mariano<sup>1,2</sup>

<sup>1</sup> Departamento de Física, Facultad de Ciencias Exactas, Universidad Nacional de La Plata, C.C. 67, 1900 La Plata, Argentina

<sup>2</sup> Instituto de Física La Plata, CONICET, 1900 La Plata, Argentina

E-mail: [barbero@fisica.unlp.edu.ar](mailto:barbero@fisica.unlp.edu.ar)

Received 5 March 2015, revised 24 July 2015

Accepted for publication 30 July 2015

Published 9 September 2015



CrossMark

## Abstract

It is a well known fact that when a resonance (R) is produced and decays, its unperturbed propagator will be singular at  $p^2 = m_R^2$  when it appears in an s-type Feynman pole graph. Nevertheless this is not a problem, since it must be dressed by the successive re-interactions of the resonance with itself to all orders through the non-pole T-matrix, which we include in this work for the self-energy one-loop pion–nucleon contributions. Recently, we have shown that within the one-loop approximation for the absorptive part it is possible to justify the use of the complex-mass description  $m \rightarrow m - i\Gamma/2$  over the unperturbed propagator, adopted in previous calculations to treat pion–nucleon elastic and radiative scattering, and photo and weak pion production in the resonance region. Here we discuss the limits of the validity of this approximation, since in actual calculations we must go over this range. We show that, when the resonance energy is increased above  $\sqrt{p^2} \sim 1400$  MeV, this approach becomes invalid and an alternative approximation should be considered. In addition, we discuss the usual energy dependent width approximation, present in several actual isobar models used to analyze the last neutrino scattering experiments, and show that also it could be inappropriate.

Keywords: delta resonance, dressed propagator, complex mass scheme

## 1. Introduction

Several reactions on free nucleons involving leptonic and hadronic probes excite the  $\Delta$  (1232 MeV) hadronic resonance as an intermediate state. This resonance, being the first excited on the nucleon, is the dominant degree of freedom in the pion ( $\pi$ )-production

processes at invariant-masses of  $\pi$ -nucleon ( $N$ )  $\Delta$  decaying pairs in the resonance region ( $m - \Gamma, m + \Gamma$ ) until  $\sim 1.4$  GeV. A consistent model for including the  $\Delta$  was successfully used for describing elastic and radiative  $\pi N$  scattering [1],  $\pi$ -photoproduction off nucleons [2] and the single  $\pi$ -production in charged and neutral current neutrino ( $\nu$ )- $N$  scattering reactions [3], in that region. Also, several parameters of this resonance such as its mass  $m$ , the  $\pi N \Delta$  coupling constant  $g$ , the width  $\Gamma$ , the magnetic dipole moment  $\mu$ , the magnetic  $G_M(Q^2 = 0)$  and electric  $G_E(Q^2 = 0)$  form factors and the axial coupling constant  $C_5^V$ , were adjusted consistently and with reasonable precision within this model. When we go over the before mentioned energy range we must analyze both the validity of the model used to treat the  $\Delta$  and the effect of more energetic resonances appearing, many of them also with spin  $3/2$ . As an example, we consider here the  $\pi N$  scattering process. The idea is not to discuss in detail the physics at energies above the  $\Delta(1232)$  resonance for this process, but only to analyze the behavior of the  $\Delta$  propagator at higher energies. We will try to find a well-behaved isobar model to include the  $\Delta$  resonance in that region without modifying the low energy description in order to use with confidence the already adjusted parameters. It is interesting to mention here that this will be useful for other reactions including the  $\Delta$ , like neutrino scattering, where a not detailed analysis of the approaches used to include the resonance has been performed and extracted parameters are considered reliable. In addition, it is important to know the high energy behavior of the  $\Delta$  contribution to introduce later more energetic resonances which could to hide inappropriate aspects of the model used to include them.

The paper is organized as follows: in section 2 we present different approximations for the  $\Delta$  propagator; in section 3 we present and discuss the effect of these approximations on the  $\pi N$  cross section; section 4 exhibits our final conclusions.

## 2. The $\Delta$ resonance propagator

Any amplitude describing the production and decay of resonances, containing resonant and background contributions, should fulfil covariance, unitarity and satisfy gauge invariance in the presence of electromagnetic interactions. The first requirement is fulfilled since we build the amplitudes from effective covariant chiral Lagrangians. The second one comes from the property  $SS^\dagger = I$  for the S-matrix which in time leads to the requirement for the amplitude  $\mathcal{M}$

$$2 \operatorname{Im} [\mathcal{M}(i \rightarrow i)] = \sum_X \int d\Pi_{\text{LIPS}}^X \mathcal{M}(i \rightarrow X) \mathcal{M}^\dagger(X \rightarrow i), \quad (1)$$

where

$$d\Pi_{\text{LIPS}}^X = (2\pi)^4 \delta^4(P_i - \sum p_j = P_X) \Pi_{\text{final } j \text{ in } X} \frac{d^3 p_j}{(2\pi)^3} f(E(\mathbf{p}_j)), \quad (2)$$

with  $f(E(\mathbf{p}_j)) = \frac{1}{2E(\mathbf{p}_j)}$  for bosons and  $f(E(\mathbf{p}_j)) = \frac{m_j}{E(\mathbf{p}_j)}$  for fermions, with  $i$  being a two particle initial state and  $X$ , with  $j = 1, 2, \dots$  particles, all possible final states. It is important to mention that (1) must be fulfilled ‘order by order’ in a perturbative scheme. Finally, the electromagnetic gauge invariance in processes involving the  $\Delta\gamma\Delta$  vertex [4] and all other contributions coming from attaching a photon by minimal coupling to each particle line and vertex in the amplitude, is guaranteed when the Ward–Takahashi identity between the  $\Delta$  radiative vertex  $\Gamma_{\Delta\gamma\Delta}^{\mu\nu}$  and propagator  $G^{\mu\nu}(p^2)$

$$i(p' - p)_\alpha \Gamma_{\Delta\gamma\Delta}^{\mu\nu\alpha} = G^{-1\mu\nu}(p') - G^{-1\mu\nu}(p), \quad (3)$$

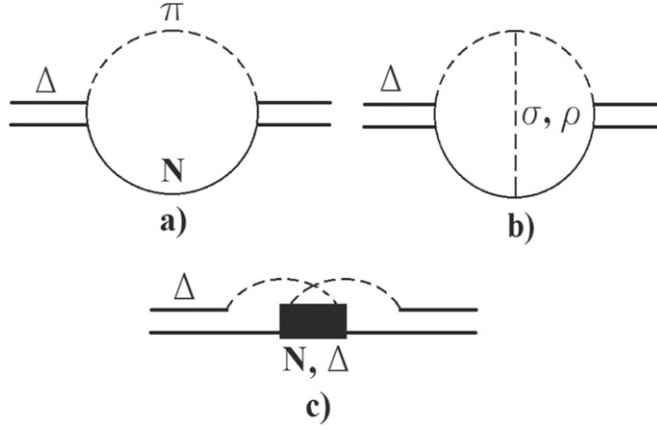


**Figure 1.** Contribution of the  $\pi N$  one bubble to the  $\Delta$  self-energy (1 a)). One meson exchange, and cross- $N$  and  $\Delta$  contributions (1 b) and 1 c) graphs respectively) to the  $\Delta$  self-energy.

is fulfilled, where  $G^{-1\mu\alpha}(p)G_{\alpha\nu}(p) = g_{\nu}^{\mu}$ , and  $\Gamma_{\Delta\gamma\Delta}$  is obtained from the minimal replacement in the kinetic  $\Delta$  Lagrangian (see [4]).

The unperturbed  $\Delta$  propagator

$$G_0^{\mu\nu} = \frac{\not{p} + m}{p^2 - m^2} \left\{ -g^{\mu\nu} + \frac{1}{3}\gamma^{\mu}\gamma^{\nu} + \frac{2}{3m^2}p^{\mu}p^{\nu} - \frac{1}{3m}(p^{\mu}\gamma^{\nu} - \gamma^{\mu}p^{\nu}) - \frac{2(\not{p} - m)}{3m^2}[\gamma^{\mu}p^{\nu} - p^{\mu}\gamma^{\nu} + (\not{p} + m)\gamma^{\mu}\gamma^{\nu}] \right\}, \quad (4)$$

satisfies the identity (3), but being singular at  $p^2 = m^2$  it should be dressed by the inclusion of a self-energy ( $\Sigma$ ) [2] giving to it a width corresponding to an unstable particle. This self-energy (where usually only Born interaction terms are considered) could include the lowest order  $\pi N$  one-loop contribution (figure 1(a)) as well as other higher order  $\pi N$  irreducible scattering non-pole (NP) terms (figures 1(b)) and (c) consistent with the  $\pi N$  scattering amplitude [1]. The dressed propagator can be then obtained by solving the Schwinger–Dyson equation

$$G^{\mu\nu}(p) = G_0^{\mu\nu}(p) - G_0^{\mu\nu'}(p)\Sigma_{\nu'\mu'}(p)G^{\mu'\nu}(p), \quad (5)$$

or equivalently for the inverse propagators

$$(G^{-1})^{\mu\nu}(p) = (G_0^{-1})^{\mu\nu}(p) - \Sigma^{\mu\nu}(p). \quad (6)$$

This propagator, including one-loop self-energy contributions (figure 1(a)), has been deduced in [5] together with a discussion about some approximated forms and reads

$$\begin{aligned}
G^{\mu\nu}(p) = & \frac{\tilde{m} + \not{p}}{\tilde{m}^2 - p^2} (\mathcal{P}^{3/2})^{\mu\nu} \\
& + \frac{1}{2} \left[ \frac{2\tilde{m} - 2\sqrt{p^2} + A_+}{-\tilde{m}^2 + X_+} + \frac{2\tilde{m} + 2\sqrt{p^2} + A_-}{-\tilde{m}^2 + X_-} \right] (\mathcal{P}_{11}^{1/2})^{\mu\nu} \\
& + \frac{1}{2\sqrt{p^2}} \left[ -\frac{2\tilde{m} - 2\sqrt{p^2} + A_+}{-\tilde{m}^2 + X_+} + \frac{2\tilde{m} + 2\sqrt{p^2} + A_-}{-\tilde{m}^2 + X_-} \right] \not{p} (\mathcal{P}_{11}^{1/2})^{\mu\nu} \\
& + \frac{1}{2} \left[ \frac{3 \frac{J_3 - \sqrt{p^2} J_4}{1 - J_2}}{-\tilde{m}^2 + X_+} + \frac{3 \frac{J_3 + \sqrt{p^2} J_4}{1 - J_2}}{-\tilde{m}^2 + X_-} \right] (\mathcal{P}_{22}^{1/2})^{\mu\nu} \\
& + \frac{1}{2\sqrt{p^2}} \left[ \frac{3 \frac{J_3 - \sqrt{p^2} J_4}{1 - J_2}}{-\tilde{m}^2 + X_+} - \frac{3 \frac{J_3 + \sqrt{p^2} J_4}{1 - J_2}}{-\tilde{m}^2 + X_-} \right] \not{p} (\mathcal{P}_{22}^{1/2})^{\mu\nu} \\
& + \frac{\sqrt{3}}{2} \left[ \frac{\tilde{m} - \left( \frac{J_1 + \sqrt{3} J_7}{1 - J_2} \right)}{-\tilde{m}^2 + X_+} - \frac{\tilde{m} - \left( \frac{J_1 - \sqrt{3} J_7}{1 - J_2} \right)}{-\tilde{m}^2 + X_-} \right] \left[ (\mathcal{P}_{21}^{1/2})^{\mu\nu} + (\mathcal{P}_{12}^{1/2})^{\mu\nu} \right] \\
& - \frac{\sqrt{3}}{2\sqrt{p^2}} \left[ \frac{\tilde{m} - \left( \frac{J_1 + \sqrt{3} J_7}{1 - J_2} \right)}{-\tilde{m}^2 + X_+} + \frac{\tilde{m} - \left( \frac{J_1 - \sqrt{3} J_7}{1 - J_2} \right)}{-\tilde{m}^2 + X_-} \right] \\
& \times \not{p} \left[ (\mathcal{P}_{21}^{1/2})^{\mu\nu} - (\mathcal{P}_{12}^{1/2})^{\mu\nu} \right], \tag{7}
\end{aligned}$$

where

$$\begin{aligned}
X_{\pm} & \equiv \frac{2m \left( J_1 + J_3 \pm \sqrt{3} J_7 \mp \sqrt{p^2} J_4 \right) + 2\sqrt{p^2} \left( \mp J_3 + \sqrt{p^2} J_4 \right) + J_1^2}{(1 - J_2)^2}, \\
A_{\pm} & \equiv \frac{3 \left( J_5 \pm \sqrt{p^2} J_6 \right) - 2 \left( J_1 \pm \sqrt{p^2} J_2 \right)}{1 - J_2}, \tag{8}
\end{aligned}$$

and the effective mass is given by

$$\tilde{m} \equiv \frac{m + J_1}{1 - J_2}. \tag{9}$$

The coefficients  $J_i$  are functions of  $\sqrt{p^2}$  and the  $S = 1/2, 3/2$  spin projectors  $\mathcal{P}_{ij}^S$  are defined in [5]. It is important to note that this expression is valid for complex  $J_i$ , that is, when the real and the absorptive contributions of the self energy are considered. Here we mention that:

1) It is well known that the real contributions to the loop are divergent and require a renormalization procedure, including counterterms proportional to each one of the  $\mathcal{P}_{ij}^S$  projectors. This is by no means a trivial task and is out of the scope of this article. In place of this, we have used dispersion relations to estimate these real contributions, as described below. The dressed mass  $m$  in equations (7)–(9) should satisfy the renormalization condition

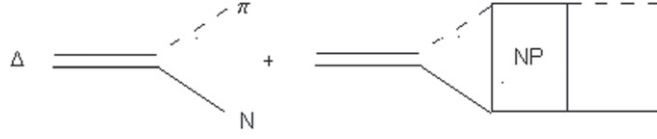


**Figure 2.** Dressing of  $\Delta \rightarrow \pi N$ . In the NP box we must include one meson exchange, and cross-nucleon and  $\Delta$  rescattering contributions as in figures 1(b) and (c).

$$m_0 - m + \text{Re} \left[ J_1(\sqrt{p^2}) + \sqrt{p^2} J_2(\sqrt{p^2}) \right] \Big|_{p^2=m^2} = 0, \quad (10)$$

with  $m_0$  being the bare  $\Delta$  mass. Instead of solving this equation to find  $m$ , we have adjusted  $m$  by fitting to the experimental  $\pi N$  cross section [8].

2) Firstly, we have only considered the absorptive contribution to the one-loop self-energy in the rest of the propagator. For this, all the  $J_i$  in equations (7)–(9) are taken as pure imaginary and their expressions are given in [5].

The dressed propagator within this approach will be named ‘EXACT’ in the rest of the paper. It is important to mention that at this stage the treatment we give to the real part of the self-energy is similar to that achieved in [9], where the self-energy is taken as its on shell value and the propagator is reduced to the 3/2 sector, as well as in [10], where the 3/2 part of the propagator is included within a chiral perturbation framework. Also, we mention [11] where a many-body approach to the  $\Delta$  self-energy is developed within a nuclear matter framework. There, the energy dependence of the real part is considered except for the nuclear matter propagator and not for the free one, with the zero density contributions subtracted since the authors assume a  $\Delta$  renormalized propagator in free space with its physical mass.

Another important point to mention here is with regard to gauge invariance. Since  $G_0$ , which corresponds to  $\Sigma \equiv 0$  in (6), satisfies the Ward identity (3) it is clear that the exact dressed propagator (7) does not. To render again electromagnetic gauge invariance we must to add vertex corrections representing the coupling of the photon in ‘all’ ways to the self-energy contribution depicted in graph 1 a), a very lengthly calculation in our case. This procedure has been developed in [10, 12] (and references therein) for the propagator in the 3/2 sector within a chiral perturbation framework. Nevertheless, as we will see, it is possible to simplify this situation (as done for other unstable particles [6]) around the resonance region to get a gauge invariant amplitude in the presence of finite width effects.

Neglecting terms of  $O(g^4)$  and of  $O((m - \sqrt{p^2})g^2)$  which are expected to be very small in the resonance region ( $\sqrt{p^2} \approx m$ ) in equations (7), (8) and (9), one gets [5]

$$G^{\mu\nu} = \frac{\tilde{m} + \not{p}}{\tilde{m}^2 - p^2} (\mathcal{P}^{3/2})^{\mu\nu} - \frac{2}{\tilde{m}^2} (\tilde{m} + \not{p}) (\mathcal{P}_{11}^{1/2})^{\mu\nu} + \frac{\sqrt{3}}{\tilde{m}\sqrt{p^2}} \not{p} \left[ (\mathcal{P}_{21}^{1/2})^{\mu\nu} - (\mathcal{P}_{12}^{1/2})^{\mu\nu} \right], \quad (11)$$

with ( $s \equiv p^2$ )

$$\tilde{m} \approx m - i \frac{\Gamma(s)}{2}, \quad (12)$$

and where the energy-dependent  $\Delta \rightarrow N\pi$  decay width is defined as:

$$\Gamma(s) = \frac{g^2}{4\pi} \left( \frac{(\sqrt{s} + m_N)^2 - m_\pi^2}{48 s^{5/2}} \right) \lambda^{3/2}(s, m_N^2, m_\pi^2), \quad (13)$$

with  $\lambda(x, y, z) = x^2 + y^2 + z^2 - 2xy - 2xz - 2yz$ . For the sake of completeness, we mention that up to this moment we have considered only the dressing of the  $\Delta$  propagator. Nevertheless, analyzing the formal scattering T-matrix calculations [2], one can realize that the  $\Delta \rightarrow \pi N$  vertex should be also dressed by NP  $\pi N$  rescattering terms like those that built figures 1(b) and (c) and as shown schematically in figure 2. This of course generates a dependence on  $s$  in the vertex, or equivalently an effective coupling constant  $g(s)$ , due to the intermediate  $\pi N$  propagator in the second graph of figure 2.

Now, we consider the formal limit of massless  $N$  and  $\pi$  in the loop contribution to  $\tilde{m}$  [6] and in the dressed  $\pi N \Delta$  vertex. We assume within this formal limit that the dressing gives a dependence  $g(s) = \frac{\tilde{g}}{\sqrt{s}}$ , with adimensional  $\tilde{g} \equiv a g_0$ , with  $g_0$  being the bare  $\pi N \Delta$  coupling constant and  $a$  a constant to fit since we are avoiding the direct calculation of the momentum integral present in the vertex correction. Thus, we derive from (13) the following approximated expression for the effective mass

$$\tilde{m} \simeq m - i \frac{\Gamma}{2}, \quad (14)$$

with the width,

$$\Gamma = \Gamma^{\text{CMS}} \left( 1 + \frac{s^{1/2} - m}{m} \right), \quad \Gamma^{\text{CMS}} = \frac{\tilde{g}^2 m}{192\pi}. \quad (15)$$

In the  $s \approx m^2$  region we have a constant width  $\Gamma_\Delta \approx \Gamma_\Delta^{\text{CMS}}$ , where now  $\Gamma^{\text{CMS}}$  will be fitted in place of  $a$ . This is the so-called complex-mass scheme (CMS) [4]. Within this prescription we can rewrite finally the propagator (using the expressions for the projectors) as

$$G^{\mu\nu} = \frac{\not{p} + \tilde{m}}{p^2 - \tilde{m}^2} \left\{ -g^{\mu\nu} + \frac{1}{3} \gamma^\mu \gamma^\nu + \frac{2}{3\tilde{m}^2} p^\mu p^\nu - \frac{1}{3\tilde{m}} (p^\mu \gamma^\nu - \gamma^\mu p^\nu) - \frac{2(\not{p} - \tilde{m})}{3\tilde{m}^2} [\gamma^\mu p^\nu - p^\mu \gamma^\nu + (\not{p} + \tilde{m}) \gamma^\mu \gamma^\nu] \right\}, \quad (16)$$

which consists in replacing  $m \rightarrow m - i\Gamma^{\text{CMS}}/2$  in the unperturbed  $G_0$  one. As a result, the transition amplitude has a pole located at the complex-mass position and is no longer singular. In addition, the CMS propagator  $G = G_0(m \rightarrow m - i\Gamma^{\text{CMS}}/2)$  satisfies the Ward identity (3) like  $G_0$  before, assuring the gauge invariance of the radiative amplitude. As previously mentioned, we have successfully used the CMS prescription to introduce the finite width of the  $\Delta$  for describing elastic and radiative  $\pi N$  scattering [1],  $\pi$ -photoproduction [2] and weakly charged and neutral current  $\nu N$  scattering production [3], determining several parameters of the  $\Delta$  resonance within a consistent model built with a resonant amplitude plus the tree-level nonresonant background.

Now, we are interested in processes of  $\pi$ -production in  $\nu$ -nucleus (A) scattering where the invariant mass of the final  $\pi N$  pair is around 1700 MeV for the peak of the neutrino flux energy distribution [7, 8], and higher than this value for the MinervA experiment [13]. This encourages us to analyze the behavior of the CMS approximation for higher energies, comparing its predictions with those obtained with the calculation based on the EXACT

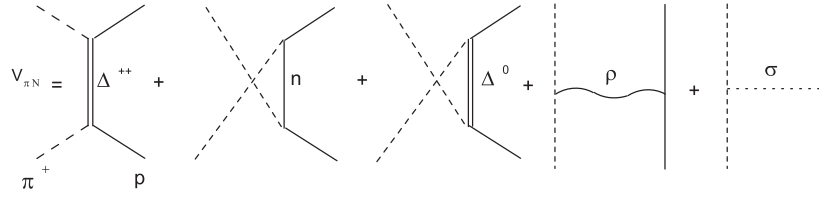


**Figure 3.** Born amplitude for  $\pi N$  scattering.

propagator previously presented. Advancing our results, we will see that the CMS approximation diverges from the data when we go above the  $\Delta$  region. Otherwise, the EXACT propagator given in equation (7) without approximations but with  $g \simeq g_0$  in  $\tilde{m}$ , reproduces poorly the low energy data when the values of  $g_0$  and  $m$  fitted with the CMS are used, but behaves properly at high energies. The idea will be then to develop an intermediate approximation that coincides with the CMS at low energies with a better behavior when the  $\pi N$  invariant mass grows. This will be called the ‘EXCMS’ dressed propagator and corresponds to the exact expression (7), but with the assumptions (14) and (15) for the effective mass. For completeness, in the next section we also estimate the effects of  $\text{Re}(J_i)$ ,  $i = 1, \dots, 7$ , by using the dispersive relations (PV denotes the principal value)

$$\text{Re}[J_i(p^2)/p^2] = \frac{1}{\pi} \text{PV} \left( \int_{(m_\pi+m_N)^2}^{\infty} \frac{\text{Im}[J_i(s)/s]}{(s-p^2)} ds \right). \quad (17)$$

Finally, we mention another approach used in several reports [14–16]. That is to use the expression (16) for the propagator with  $\tilde{m}$  not in every place but only in the singular denominator (this causes a violation of (3) still with a constant width) and with an energy dependent width (EDEPW) obtained from (13) leading to the approximation

$$(\sqrt{s} + m_N)^2 - m_\pi^2 = \sqrt{s} m_N [(\sqrt{s} - m_N)/m_N + (m_N - \sqrt{s})/\sqrt{s} + m_\pi^2/\sqrt{s} m_N + 4] \approx 4\sqrt{s} m_N$$

valid only in the  $\Delta$  region. In addition, some of those studies confuse the first line in equation (16) with  $\mathcal{P}_{3/2}$ , really it is  $\mathcal{P}_{3/2}(p^2 = m^2)$ , and drop the second line, taking  $p^2 = \tilde{m}^2 = m^2$ . We call this approach EDEPON (energy dependent on-shell). Finally, the question about the unitarity of the several approximations also will be addressed below.

### 3. Results and discussion

To compare the behavior of the different models we choose the simplest reaction involving the excitation of the  $\Delta$ , that is the  $\pi^+ p$  scattering up to energies  $T_{\pi\text{lab}} = p_\pi^2/2 + m_\pi \simeq 900$  MeV ( $\sqrt{s}_{\pi N} = 1700$  MeV) covering also the energy range of the final  $\pi N$  pair but now for weak  $\pi$  production reactions at  $E_\nu \sim 1$  GeV. Our model will include the Born amplitudes shown in figure 3 built by a resonant (R) pole term (first graph) plus a background (B) with NP contributions (second to fourth graphs).

It is very important to mention that in the R contribution, higher order terms will be generated through the use of the perturbed propagator, but the B one will be kept at tree level. Then, this model is far from one devoted to fixing scattering phase-shifts with good precision. Nevertheless, these kind of isobar models are actually adopted for describing elementary



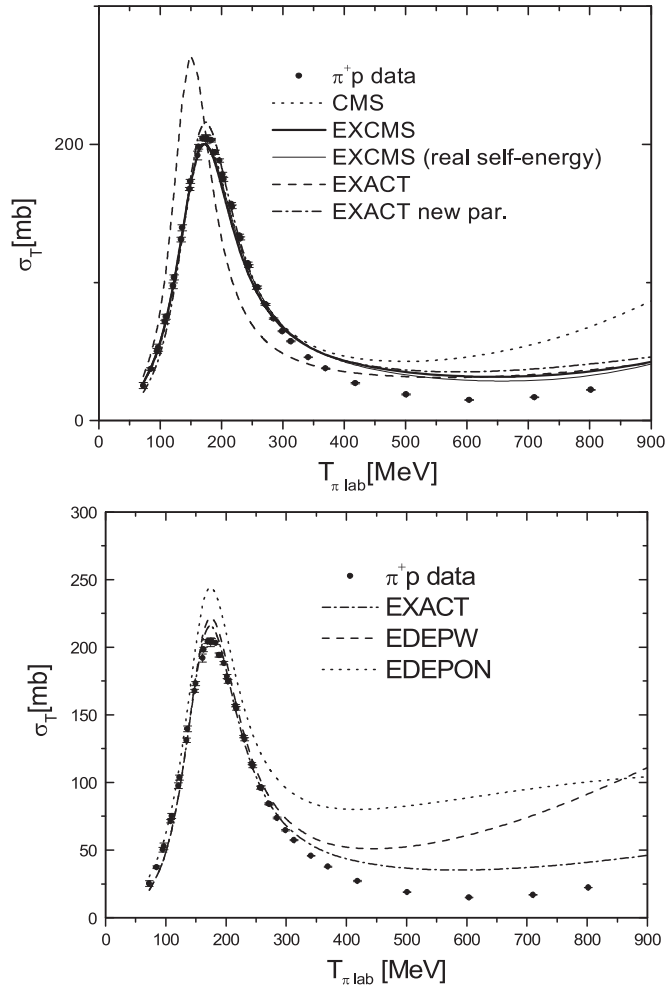


**Figure 4.** Total cross section of  $\pi^+p$  scattering for different versions of the propagator. Upper panel CMS, EXCMS and EXACT with the same CMS fitted parameters and the EXACT with the new fitted parameters. Lower panel EXACT, EDEPW and EDEPON with the same new fitted parameters. Data is taken from the database at the Center of Nuclear Studies, Department of Physics, George Washington University.

amplitudes in  $\nu N$  scattering [3, 15, 16] and it will be crucial to analyze the behavior at the required energies.

In the upper panel of figure 4 we show the calculation of the total cross section ( $\sigma_T$ ) for the different versions of the  $\Delta$  propagator presented previously. We have used  $m = 1211.20$  MeV,  $\Gamma = 88.16$  MeV,  $g_0 = 14.46 \text{ GeV}^{-1}$  ( $f_{\pi N \Delta}/4\pi = 0.317$ ) obtained from fits to data [1] in the resonance region, working within the CMS approach. The parameters for the B contributions are also described in [1]. We show the behavior of the total cross section for the CMS, EXCMS, and EXACT approaches for the  $\Delta$  propagator in R, always with the same B and using the same CMS fitted parameters. We observe that the CMS describes the data well up to  $T_{\pi \text{ lab}} \sim 300$  MeV ( $\sqrt{s} \pi N \lesssim 1400$  MeV) over this region. This divergency originates since, to arrive to equation (16) from equation (7), we have used the approximation  $p^2 \simeq m^2$

which both affects the coefficients of the  $1/2$  propagator contributions and the energy dependence of  $\tilde{m}$ , which is no longer valid when we go far away from the resonance peak. In fact, if we observe the behavior of  $\sigma_T$  evaluated within the EXCMS scheme, in which the approximation  $p^2 \simeq m^2$  was used only to get (14) and where (15) is used, it coincides with the CMS in this energy region and shows an improvement in the behavior at energies above the peak until  $T_{\text{lab}} = 900$  MeV. Finally, using the EXACT propagator (equations (7) and (9)) with the same parameters as the CMS and EXCMS, we see that the data are not well described in the resonance region with the  $\Delta$  peak slightly shifted, and coincide with the EXCMS above this region. Thus, we should hope that including *together* the rescattering effects on B (remember that we are making a tree label treatment here) and the real part of the self-energy, which mainly affects the high energy behavior, will improve the description of the data. To get an estimate of the real part effects we have included the results obtained within the EXCMS approach using equation (17) to evaluate the real part of the  $J_i$ ,  $i = 1, \dots, 7$ . The curve is shown in figure 4 as EXCMS (real self-energy). As can be seen, one gets a small improvement, indicating that the rescattering effects on B and the interference with the resonance could be important. This additional improvement is by no means trivial to achieve and we feel that it is not crucial at the moment for making a comparison with the other approaches EDEPW and EDEPON used mostly in the literature, mainly because they do not include the effects mentioned above.

From this, we conclude that the overvaluation of the data over the resonance region could be attributed to the tree label treatment of the B amplitude. Now in the EXACT calculation, the width is not a parameter to adjust and the real effective mass should not be the same, since we are using (9) and not (15), with  $g = g_0$  without including vertex corrections as explained before. If we try to make a fit with the EXACT propagator we get  $m = 1235.48$  MeV,  $g = 15.32 \text{ GeV}^{-1}$  ( $f_{\pi N \Delta}/4\pi = 0.366$ ) and  $g_\sigma/4\pi = 0.329$  for  $m_\sigma = 650$  MeV (the most unknown meson in the model) where again, as was seen before [1], the sensitivity to  $m_\sigma$  was analyzed. As can be seen, the new fit improves the description, but still the calculation with EXCMS is closer to the data. In the lower panel of figure 4 we compare the EXACT calculation with the above mentioned EDEPW and EDEPON approaches, this last one assumed by other authors [15]. We use the new fitted parameters with the EXACT propagator, which are very close to that assumed in the aforementioned work. As can be seen, this EDEPW approach, in spite of being close to the EXACT in the resonance region, diverges for higher energies due to the same reasons as before, the approximations in the  $1/2$  sector coefficients. The EDEPON description is the worst, since the cutting done in equation (16) through out both, contributions from the  $3/2$  and  $1/2$  sector that are important in the peak region and in the determination of the R-B interference. More sensitivity to the data is presented in the calculation of the differential cross section. In figure 5 we show it for different precise  $T_{\pi\text{lab}}$  energies and for several approaches. We can see again that within our rudimentary model for the B amplitude (which does not include rescattering) the best description is within the EXCMS approach. Also, for higher energies both the EXACT and the EXCMS depart from the data but are much closer than the other approaches.

On the other hand, it is supposed that a better description of the data corresponds with the better fulfilling of unitarity in the amplitude. Now, we wish to discuss the EXACT, EXCMS, EDEPW and EDEPON approaches from the point of view of unitarity (for the CMS this was discussed before in [1]). It is understandable that if we only consider the pole- $\Delta$  amplitude (left graph in figure 3) together with the EXACT propagator (7), equation (1) with  $X = \pi N$  is satisfied order by order in the strong  $\pi N \Delta$  interaction, since the imaginary part of any intermediate loop (see figure 1(a)) of an  $n$ -order amplitude gives the same contribution as  $|\mathcal{M}|^2$  on the right side for an  $n/2$ -order amplitude. This will not be true for the other

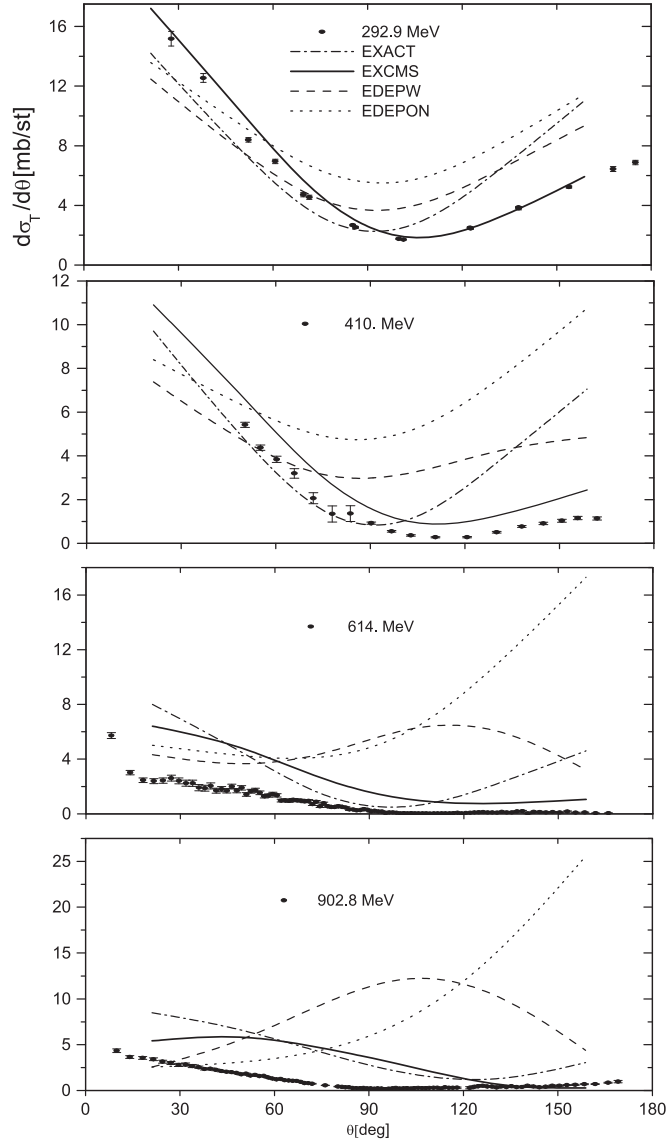


**Figure 5.** Comparison of the  $\pi^+p$  differential cross section calculated with the different approaches for the indicated  $T_{\pi\text{lab}}$  energies.

mentioned approaches since they are obtained using approximations on (7). Nevertheless, as we have included an energy dependent  $g$  in the EXCMS case, indicating that vertex corrections produced by the B contributions are also present, then the simple way to corroborate unitarity in the EXACT case is no longer valid. It would be more appropriate to analyze the unitarity of the full (R+B) amplitude. It is clear that the B amplitude is not unitary since equation (1) is not fulfilled, with this amplitude being real at tree level and certain unitarity violation will occur for the R+B amplitude. In figure 6 we show with thin lines the calculation for  $\sigma_T$  using the imaginary part on the left-hand side of equation (1) and with thick lines the right-hand one. As we can see, unitarity is not fulfilled in any of the approximations, but

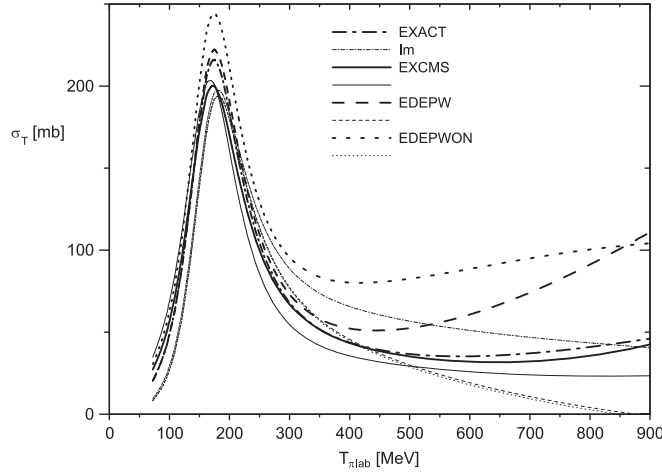


**Figure 6.** Comparison of the  $\pi^+p$  total cross section calculated using the right-hand side of equation (1) (tick lines) with those calculated with the left-hand one (thin lines) indicated with the legend ‘Im’. We analyze the EXACT, EXCMS, EDEPW, and EDEPON approximations with the same NR background.

the closest results between both sides of equation (1) are obtained within the EXCMS case. Within the EXACT approach in spite of having unitarity of the R amplitude the R+B is not unitary since we do not consider vertex corrections and also due to the real character of the B amplitude. The lack of unitarity for EDEPW is worse with the maximum violation seen within the EDEPON approach.

Finally, it is important to make a comment regarding the cross- $\Delta$  contribution (third graph in figure 3). As mentioned previously, the growth of the cross section for the CMS, EDEPW and EDEPON approaches is due to the approximations achieved for the coefficients of the  $1/2$ -sector in equation (7). Then, it is possible to think that a good approach would be to directly remove the spin  $1/2$  part of the propagator. As for the cross- $\Delta$  contribution is  $p^2 < m^2$  and the self-energy one-loop contribution is zero (see [5]) this amplitude is calculated with the unperturbed (4) propagator equivalent to (7) with  $\Sigma = 0$ . Now, the projectors in (7) have  $p^2$  denominators [5] that could be zero (generating singularities) for the mentioned cross- $\Delta$  graph, and without a delicate balancing between the  $3/2$  and  $1/2$  contributions the non-singular (4) form will not be reached. If we remove the  $1/2$  sector then (7) transforms into

$$G^{\mu\nu}(p) = \frac{\tilde{m} + \not{p}}{\tilde{m}^2 - p^2} (\mathcal{P}^{3/2})^{\mu\nu},$$

which can be singular when  $p^2 = 0$  [17]. Then it is not possible to remove the  $1/2$  sector.

#### 4. Final remarks

In summary, we have discussed here the limits of validity of the CMS approximation, already used to fit several  $\Delta(1232 \text{ MeV})$  parameters from data in the resonance region. It is shown that due to the approximations assumed in the EXACT propagator to get the approximated CMS one, this can be applied with confidence around the resonance region. In order to choose the best model for energies over this limit, we have performed an analysis of the  $\pi N$

scattering cross section with different approaches for the  $\Delta$  propagator, some of them already used in the literature, but perhaps not well analyzed in this range. We have analyzed the unitarity condition in each case, and we have found the so called EXCMS results to be the most adequate. Also we have estimated the effect of considering the energy dependence of the real part of the coefficients of the self-energy within this approach, which improves the result but not enough to avoid discrepancies with data. Although it is not possible fulfil gauge invariance within the EXCMS without introducing vertex corrections, it is useful since the coincidence of it with the CMS in the resonance region enables us to combine the same parameters obtained before with the CMS (where gauge invariance is fulfilled) and a good behavior at higher energies. Although the unitarity is not fulfilled due to the real background amplitude, the violation seems to be small enough to use the EXCMS approach in other reactions at the same energies. Especially in weak pion production, where in place of having two strong vertices we combine a weak and a strong one, this indicates that departure from data will be smaller. A detailed inclusion of rescattering effects in the background amplitude will be analyzed in a future contribution.

## Acknowledgments

C B and A M fellow to CONICET (Argentina) and CCT La Plata, Argentina.

## References

- [1] López Castro G and Mariano A 2001 *Nucl. Phys. A* **697** 440  
López Castro G and Mariano A 2001 *Phys. Lett. B* **517** 339
- [2] Mariano A 2007 *J. Phys. G: Nucl. Part. Phys.* **34** 1627
- [3] Barbero C, López Castro G and Mariano A 2008 *Phys. Lett. B* **664** 70  
Barbero C, López Castro G and Mariano A 2011 *Nucl. Phys. A* **849** 218
- [4] el Amiri M, Pestieau J and Lopez Castro G 1992 *Nucl. Phys. A* **543** 673
- [5] Barbero C, Mariano A and López Castro G 2012 *J. Phys. G: Nucl. Part. Phys.* **39** 085011
- [6] López Castro G and Toledo Sanchez G 2000 *Phys. Rev. D* **61** 033007
- [7] MinoBooNE Collaboration ([www-boone.fnal.gov/collaboration](http://www-boone.fnal.gov/collaboration))
- [8] T2K Collaboration (<http://t2k-experiment.org/>)
- [9] de Jong F and Malfliet R 1992 *Phys. Rev. C* **46** 2567
- [10] Pascalutsa V, Vanderhaeghen M and NanYang S 2007 *Phys. Rep.* **437** 125
- [11] Oset E and Salcedo L L 1987 *Nucl. Phys. A* **468** 631
- [12] Pascalutsa V and Vanderhaeghen M 2005 *Phys. Rev. Lett.* **94** 102003
- [13] MinervA Collaboration <http://minerva.fnal.gov/>
- [14] Fogli G L and Nardulli G 1979 *Nucl. Phys. B* **160** 116
- [15] Hernandez E, Nieves J and Valverde M 2007 *Phys. Rev. D* **76** 033005
- [16] Lalakulich O, Leitner T, Buss O and Mosel U 2010 *Phys. Rev. D* **82** 093001
- [17] Bermerrouche M, Davidson R M and Mukhopadhyay N C 1989 *Phys. Rev. C* **39** 2339